



A novel single-domain antibody multimer that potently neutralizes tetanus neurotoxin

Hans de Smit^{a,*}, Bart Ackerschott^a, Robert Tierney^b, Paul Stickings^b, Michiel M. Harmsen^c

^a R&D, Smivet B.V., Diemewei 4110, 6605XC Wijchen, the Netherlands

^b Division of Bacteriology, National Institute for Biological Standards and Control (NIBSC), MHRA, Potters Bar, Hertfordshire EN6 3QG, UK

^c Wageningen Bioveterinary Research, P.O. Box 65, 8200 AB Lelystad, the Netherlands



ARTICLE INFO

Article history:

Received 4 September 2020

Received in revised form 17 April 2021

Accepted 27 May 2021

Available online 29 May 2021

Keywords:

Tetanus antitoxin

Neurotoxin

Neutralization

VHH

sdAb

Single-domain antibody

Therapeutic antibody

veterinary biotherapeutics

ABSTRACT

Tetanus antitoxin, produced in animals, has been used for the prevention and treatment of tetanus for more than 100 years. The availability of antitoxins, ethical issues around production, and risks involved in the use of animal derived serum products are a concern. We therefore developed a llama derived single-domain antibody (VHH) multimer to potentially replace the conventional veterinary product. In total, 28 different tetanus neurotoxin (TeNT) binding VHHs were isolated, 14 of which were expressed in yeast for further characterization. Four VHH monomers (T2, T6, T15 and T16) binding TeNT with high affinity ($K_D < 1$ nM), covering different antigenic domains as revealed by epitope binning, and including 3 monomers (T6, T15 and T16) that inhibited TeNT binding to neuron gangliosides, were chosen as building blocks to generate 11 VHH multimers. These multimers contained either 1 or 2 different TeNT binding VHHs fused to 1 VHH binding to either albumin (A12) or immunoglobulin (G13) to extend serum half-life in animals. Multimers consisting of 2 TeNT binding VHHs showed more than a 10-fold increase in affinity (K_D of 4–23 pM) when compared to multimers containing only one TeNT binding VHH. The T6 and T16 VHHs showed synergistic *in vivo* TeNT neutralization and, when incorporated into a single VHH trimer (T6T16A12), they showed a very high TeNT neutralizing capacity (1,510 IU/mg).

© 2021 The Authors. Published by Elsevier Ltd. This is an open access article under the CC BY-NC-ND license (<http://creativecommons.org/licenses/by-nc-nd/4.0/>).

1. Introduction

Tetanus [1] is caused by the potent tetanus neurotoxin (TeNT) produced by *Clostridium tetani* bacteria. All mammals are sensitive to TeNT and tetanus related death rates in humans are mainly related to neonatal tetanus. Tetanus can be prevented by vaccination, nevertheless tetanus remains a danger for non-immune mammals [2,3,4].

For more than 100 years immunized animals have been bled to provide serum for the treatment of humans against tetanus [5,6]. In veterinary and human medicine, the reliable supply, the potential adverse effects after administration, and the risks of yet unknown contaminants in antitoxin derived from equine serum remain a challenge [7,8]. For these and animal welfare reasons an *in vitro* produced tetanus antitoxin is preferable. In addition, a highly specific, potent and rationally designed antitoxin could improve the clinical outcome of tetanus compared to a serum derived product [1]. The discovery of, and research into, camelid single-domain antibodies (VHHs) in the past 25 years has enabled

many medicinal applications [9]. Initiatives to develop novel antibody therapies for tetanus as well as other toxin-mediated diseases started in the 1980s–1990s [10–12] and continued using various innovative recombinant antibody technology approaches [13–17].

The mechanism of TeNT neutralization by antibodies is variable due to its complex and pH-mediated variable structure [18–20]. TeNT (150-kDa) consists of a 50-kDa light chain (LC) and a 100-kDa heavy chain (HC). The HC is composed of a 50-kDa N-terminal domain (H_N) and a 50-kDa C-terminal domain (H_C) that is referred to as tetanus toxin fragment C (TTC). The TTC fragment comprises two subdomains, H_{CN} and H_{CC} . The various domains have specific functions. The TTC fragment enables binding to gangliosides on neurons. The H_{CC} subdomain contains two ganglioside binding sites that are termed the W and R pockets. Both sites can separately bind 2 different types of gangliosides and are essential for toxicity [19,21,22]. The H_N domain is responsible for translocation of the LC into the cytoplasm by undergoing a pH-mediated conformational change [20]. Finally, the LC proteolyzes the intracellular synaptic vesicle protein synaptobrevin [23] resulting in the inhibition of neurotransmitter release into the synaptic cleft causing spastic paralysis. Many other toxins are similarly composed of 3 functional domains. Among these, the bacterial

* Corresponding author.

E-mail address: ajdesmit@smivet.com (H. de Smit).

diphtheria toxin, anthrax lethal and edema toxins, *C. difficile* toxin A and botulinum neurotoxin (BoNT) are targets for recombinant antibody therapies [24].

Most TeNT neutralizing antibodies bind TTC and block entry into neurons [25–29]. Antibodies to other parts of TeNT (e.g. LC) can provide *in vivo* protection [10,11,30]. In addition to binding at a relevant location, an affinity of less than 10 nM is desirable [27]. In addition, the potency of therapeutic antibodies as determined in a standardized *in vivo* model using official reference standards [11,17,31] is crucial to correlate results to existing treatments based on international units. Mixtures of monoclonal antibodies (mAbs) can provide a synergistic increase in potency against TeNT [10,11] or other bacterial toxins [32]. This effect has been noted after the genetic fusion of VHHs for several bacterial [14,33,34] and viral [35] targets, and can even support antigen cross-reactivity [36].

To provide an acceptable posology without both daily administration and unnecessary high dosages there is a need to prolong the short *in vivo* residence time of VHH multimers for example by inclusion of VHH domains binding to long-lived serum proteins [37,38]. This study aimed at developing a VHH multimer that can potentially neutralize TeNT. We first isolated a panel of TeNT binding VHHs based on the ability to bind to TeNT and rTTC, and to block TeNT-ganglioside receptor interaction that is mediated by TTC. Here we report the development of a bivalent, bispecific VHH multimer that can potentially neutralize TeNT *in vivo*.

2. Materials and methods

2.1. Animals

For immunization, two (animals 9236 and 9237) 2-year-old female llamas (*Lama glama*) were kept in a meadow and provided with food and water ad libitum. The study was performed under the supervision of the Animal Experimental Committee of Wageningen Bioveterinary Research in accordance with EU Directive 2010/63/EU and the Dutch Law on Animal Experiments. Permission was granted by the Dutch Central Authority for Scientific Procedures on Animals (Permit Number: AVD40100201545).

For the tetanus antitoxin potency assays, female NIH mice (NIH/OlaHsd) at 14–20 g were obtained from Envigo. Mouse studies were performed under a Project Licence granted by the UK Home Office (80/2634 or P6014F8B4) and reviewed/approved by the NIBSC Animal Welfare and Ethical Review Body. The procedure used in the mouse studies is regulated by the Animals (Scientific Procedures) Act 1986 in accordance with EU Directive 2010/63/EU. Mice were housed in groups of 4 under enriched environmental conditions, were given a pelleted diet ('RM1', LBS) and water ad libitum. Animals were health and behaviour checked at least once per day during the acclimatisation period, and up to 4 times daily whilst on test by trained and competent technical staff, with attention to the degree of paralysis of the injected hind limb.

2.2. Antigens and antibodies

TeNT was obtained from List Biological Laboratories (USA). Recombinant TTC (rTTC) was obtained from Reagent Proteins (USA). Seven TeNT mouse mAbs with TeNT neutralizing properties were obtained from commercial suppliers (Supplemental Table S1). GT1b ganglioside from bovine brain was obtained from Sigma Aldrich (USA). For use in biosensors, TeNT was biotinylated at a 1:1 weight ratio with the EZ-Link[®] NHS-PEG4-Biotinylation Kit (Pierce Biotechnology, USA).

The VHH cAb-TT2 was raised against tetanus toxoid and does not recognize the TTC fragment of TeNT [12]. It was produced in

yeast strain SU51 using plasmid pRL188 in a format suitable for VHH immobilization to solid surfaces [40], without myc tag. cAb-TT2 was purified by immobilized-metal affinity chromatography (IMAC) and biotinylated as reported [40], and was used to present TeNT in an indirect format in ELISA.

2.3. Phage display selection

Llamas were injected intramuscularly simultaneously with both a ready to use tetanus toxoid vaccine intended for use in horses (1 ml, MSD Animal Health) and rTTC at day 0, 21 and 42. The rTTC (8 µg per injection) was emulsified with either Stimune adjuvant (ThermoFisher Scientific, the Netherlands) for day 0 and 21 or with IMS1312 adjuvant (Seppic, France) for day 42. Serum samples were taken at day 0, 28 and 49. Heparinized blood samples were taken at day 28 and 49 for subsequent generation of phage display immune libraries in phagemid vector pRL144 [37,41]. The libraries were rescued using VCSM13 helper phage. Phage display selections were performed by biopanning [42] with TeNT or rTTC presented by passive adsorption. Alternatively, plates were coated with cAb-TT2 or mAb TT10 [28,39] in 50 mM NaHCO₃ buffer (pH 9.6) for presentation of captured TeNT. Bound phages were eluted by 30 min incubation at 37 °C with 1 mg/ml trypsin in phosphate-buffered saline (PBS) and transduced to *Escherichia coli* (*E. coli*) TG1 [(F' traD36 proAB lacIqZ ΔM15) supE thi-1 Δ(lac-proAB) Δ(mcrB-hsdSM)5(rK⁻mK⁻)] cells. In each selection round, a phage enzyme-linked immunosorbent assay (ELISA) was performed simultaneously with the phage display selection for evaluation of the phage display. After panning individual colonies were picked and the VHH genes were induced with 1 mM isopropyl β-d-thiogalactopyranoside.

2.4. ELISA

The procedures for ELISAs as well as a phage ELISA have been described [43]. Unless otherwise stated, high binding 96-well polystyrene plates were coated with 100 µl/well of antigen overnight at 4 °C. Plates were incubated at room temperature (RT) with 100 µl/well of suitable antibodies or VHHs which were then detected with 100 µl/well of horse radish peroxidase (HRP) conjugate. Bound HRP was detected by staining with 3,3',5,5' tetramethylbenzidine. The color reaction was stopped by addition of 0.5 M sulfuric acid (50 µl per well) the absorbance at 450 nm (A450) was measured using a Multiskan Ascent spectrophotometer (Thermo LabSystems, Finland).

2.4.1. Analysis of *E. coli*-produced VHHs

Individual *E. coli*-produced VHHs clones were screened in an ELISA with coated TeNT or rTTC (at 1 µg/ml and 4 µg/ml respectively), and with cAb-TT2 or mAb TT10 (both were coated at 1 µg/ml in 50 mM NaHCO₃ buffer (pH 9.6)) immobilised TeNT (at 1 µg/ml). Plates were incubated with VHHs present in ten-fold diluted *E. coli* culture supernatants. Bound VHH was detected using 0.5 µg/ml of anti-myc clone 9E10 mAb HRP conjugate (Roche Applied Science, Germany).

2.4.2. GT1b-TeNT inhibition ELISA

A GT1b-TeNT inhibition ELISA was performed as reported [15]. Briefly, plates were coated with 10 µg/ml GT1b ganglioside in methanol at 100 µl/well by overnight incubation at RT. All subsequent incubations were performed in PBS containing 0.5% BSA and 0.05% Tween-20 for 1 h at RT. TeNT (1 µg/ml) was preincubated with VHHs, *E. coli* culture supernatants or mAbs in 100 µl/well in a plate for 1 h at RT. Next, 90 µl was transferred to the GT1b-coated plates and incubated for 1 h at RT. Plates were then incubated with 100 µl/well of 1000-fold diluted llama 9237 serum

of day 49. Bound llama IgG was detected with 10,000-fold diluted goat anti-llama IgG-HRP conjugate (G α L-HRP, Bethyl Laboratories, USA). Control incubations of TeNT without VHHs or mAbs in wells coated with GT1b (100% binding) or in wells without GT1b coating (0% binding) were included. The average A450 value of these two control incubations represents 50% inhibition (50%-A450). A four-parameter logistic curve was fitted to absorbance and antibody concentrations using the SOFTmax Pro 2.2.1 program (Molecular Devices). The antibody concentration resulting in 50% inhibition of TeNT-GT1b interaction (IC50) was then determined by interpolating the antibody concentration resulting in an A450 value equivalent to 50%-A450.

2.4.3. Analysis of yeast-produced VHHs

Various ELISA setups were done to evaluate yeast-produced monomers and multimers. We first describe the general procedure. Antigens were coated on plates as described above for *E. coli*-produced VHHs. Plates were then incubated with two-fold VHH or mAb dilution series over 12 wells starting at a 1 μ g/ml. Biotinylated VHHs or mAbs were detected with 0.5 μ g/ml of a streptavidin HRP conjugate (strep-HRP, Jackson ImmunoResearch Laboratories Inc., USA), unlabeled VHHs were detected using 9E10-HRP or G α L-HRP, and unlabeled mAbs were detected with 2000-fold diluted rabbit anti-mouse immunoglobulin HRP conjugate (R α M-HRP). A four-parameter logistic curve was fitted to absorbance and antibody concentrations with software as described under 2.4.2 and was used to interpolate the Effective Concentration (EC) resulting in a specific A450 value for each antibody.

The EC value was interpolated at a relatively low A450 value in order to prevent that antibodies with a relatively low positive ELISA signal are scored as non-binding. The A450 values used for calculation of the EC values are indicated in the figure legends. They varied from 0.15 to 0.4 between the different ELISA setups dependent on the background and maximal A450 values observed. As compared to unlabeled antibodies, biotinylated antibodies generally gave higher maximal A450 and therefore a higher A450 value was chosen for calculation of EC values. Antibodies that do not reach the A450 value defining the EC value are given an EC value of the highest antibody concentration used (1 μ g/ml). The reciprocal EC values are reported since a high 1/EC corresponds to efficient antibody binding.

Analysis of VHH monomers or mAbs binding to TeNT was done in four ELISA setups. Plates coated with TeNT and plates with TeNT immobilised using cAb-TT2 were both incubated with dilution series of unlabeled VHHs or mAbs that were subsequently detected with 9E10-HRP or R α M-HRP. Similarly, coated plates were also incubated with biotinylated VHHs or mAbs that were subsequently detected with strep-HRP. Binding to coated rTTC was analysed by incubation of unlabeled VHH or mAb at a concentration of 1 μ g/ml without further titration. The bound antibodies were detected with 9E10-HRP or R α M-HRP, respectively, and evaluated by A450 only. Analysis of VHH multimers and several VHH monomers as control was done using two ELISA setups. Plates coated with TeNT were incubated with VHH dilution series that were subsequently detected using G α L-HRP. For analysis of bispecific binding plates were coated with either dog IgG (Jackson ImmunoResearch) or dog albumin (Molecular Innovations, Novi, MI), both at 5 μ g/ml in 50 mM NaHCO₃ buffer (pH 9.6). The albumin coated plates were subsequently incubated with dilution series of VHH multimers containing the A12 VHH or the A12 VHH monomer whereas the IgG coated plates were incubated with dilution series of VHH multimers containing the G13 VHH or all further VHH monomers as control. Plates were subsequently incubated with 0.25 μ g/ml biotinylated TeNT and strep-HRP.

2.4.4. ELISA for VHH binning

The ability of VHHs and mAbs to bind independent antigenic sites of TeNT was studied by blocking/competition ELISA using biotinylated VHHs and mAbs (Table S1). ELISAs were performed using 0.5 μ g/ml TeNT for coating. The optimal concentration of biotinylated VHH or mAb for competition was first determined by titration of biotinylated VHH or mAb without competition. A biotinylated VHH or mAb concentration was used that provided about 80% of the maximal absorbance value observed with the highest VHH or mAb concentration analyzed. For competition unlabeled VHHs or mAbs were used at a concentration of 5 μ g/ml. TeNT coated plates were first incubated with the unlabeled VHH or mAb in 90 μ l/well for 30 min (blocking step). 10 μ l biotinylated VHH or mAb was added and incubated for another 30 min (competition step). In the ELISAs using biotinylated T2L and T3L, TeNT was captured with cAb-TT2. A control without antigen and a control without biotinylated VHH or mAb was included. Bound biotinylated VHH or mAb was detected by incubation with 0.5 μ g/ml streptavidin-HRP conjugate. The % inhibition of antigen binding due to a competing VHH was calculated as $100 - 100 \cdot ([A450 \text{ with competing VHH or mAb}] - [A450 \text{ without Ag coating}]) / ([A450 \text{ without competing VHH or mAb}] - [A450 \text{ without Ag coating}])$.

2.5. VHHs sequences

The VHH encoding regions of selected clones (coded T#) were sequenced as reported [37] and aligned according to the IMGT numbering system [44] of the mature VHH encoding region, ending at sequence VTSS. VHHs were classified into CDR3 groups based on having identical CDR3 length and at least 65% sequence identity in CDR3.

2.6. Production of VHHs

2.6.1. Production of monomers

TeNT binding monomers as well as control VHHs - A12L binding to animal serum albumin and G13L binding to animal immunoglobulin [45] - were produced by secretory yeast expression using plasmid pUR4585 [37]. The produced VHHs have C-terminal c-myc and H6-tags and are indicated by the suffix "L". VHH T15L-3FW4M is derived from T15L containing mutations K120Q, I122T and L123Q in framework region 4 to increase the yeast production level [49]. To produce T15L-3FW4M, a synthetic PstI-BstEII fragment encoding T15L plus mutations was inserted into pUR4585. The BstEII site required for subcloning was lacking in T16, T20, T25 and T34. Therefore, this site was silently introduced by producing synthetic PstI-BstEII fragments and inserted into pUR4585. pUR4585-derived plasmids were introduced into *Saccharomyces cerevisiae* strain W303-1a (ATCC number 208352) by selection for the auxotrophic leu2 marker.

VHH production and purification was performed as reported [37]. Purified VHHs were concentrated and buffer exchanged to PBS by use of Amicon Ultra 3-kDa molecular weight cut off centrifugal concentration devices (Millipore, USA). The concentration was determined using the Biorad (USA) protein assay and a bovine IgG standard.

2.6.2. Production of multimers

VHH multimers were produced by MIRY integrants using plasmid pRL44 in yeast strain SU50 [46]. In total 11 plasmids (Table 1) were generated that encode multimers composed of genetic fusions of TeNT binding T-VHHs with either the albumin binding VHH A12 or the IgG binding VHH G13 [45]. A mutant of T16 with the additional mutation L123Q (T16-L123Q) was used for multimer construction. Bispecific VHH dimers were linked with a (G4S)2

Table 1
Plasmid construction and yeast production level of VHH multimers.

Yeast expression plasmid ^a	Multimer VHH description ^a	VHH name	Yeast VHH production level ^b (mg/L)	Predicted MW (dalton)
pRL489	SVT6-GS2-SVA12M2-H6	T6A12	11	30,180
pRL490	SVT6-GS3-SVT16-L123Q-GS2-SVA12M2-H6	T6T16A12	10	44,990
pRL493	SVT2-GS2-SVA12M2-H6	T2A12	1	29,065
pRL494	SVT15-3FW4M-GS2-SVA12M2-H6	T15A12	34	28,739
pRL495	SVT16-L123Q-GS2-SVA12M2-H6	T16A12	99	29,192
pRL496	SVT2-GS2-SVG13M4-H6	T2G13	17	27,968
pRL497	SVT6-GS2-SVG13M4-H6	T6G13	1	29,083
pRL498	SVT15-3FW4M-GS2-SVG13M4-H6	T15G13	41	27,643
pRL499	SVT16-L123Q-GS2-SVG13M4-H6	T16G13	97	28,095
pRL505	SVT6-GS3-SVT15-3FW4M-GS2-SVA12M2-H6	T6T15A12	3	44,537
pRL506	SVT15-3FW4M-GS3-SVT6-GS2-SVG13M5-H6	T15T6G13	5	43,411

^a Nomenclature earlier used in patent application [45]. The name reflects the order of the protein domains present in the multimers from N- to C-terminus, where L123Q represents a mutation in (SV)T16 and 3FW4M represents 3 mutations in FW4 region of (SV)T15.

^b The production level in baker's yeast was calculated from the yield of purified VHH from 0.5 L shaker flask cultures.

linker (GS2) derived from pRL144 [37]. In the case of a bivalent bispecific VHH trimer, the N-terminal VHH was linked to the middle VHH via a (G4S)3 linker (GS3) as reported [47] and the middle and C-terminal VHHs were linked with a GS2 linker. The C-terminal VHH of each multimer was given an H6-tag followed by a double stop codon and HindIII restriction site.

Synthetic SacI-HindIII fragments were subcloned into pRL44 [46] using SacI and HindIII sites. Strain SU50 (MATa; cir^o; leu2-3,-112; his4-519; can1) was transformed with the 11 HpaI-linearized plasmids (Table 1) by electroporation and leu + auxotrophs were selected. A single colony-purified transformant was induced for expression (0.5 L shaker flask) and VHH was purified from supernatant by IMAC. VHH multimers were further purified by cation exchange chromatography on an SP sepharose column as reported [48], with slight modifications. VHH was eluted with a step gradient of 0.1, 0.2, 0.4, 0.6, 0.8 and 1 M NaCl in binding buffer. Eluted VHH was concentrated and buffer exchanged to PBS as described above. The concentration was determined using the bicinchoninic acid assay (BCA, Thermo Fisher Scientific) and a bovine serum albumin standard (Thermo Fisher Scientific).

2.6.3. SDS PAGE analysis and Western blotting

VHHs were analyzed by reducing SDS-PAGE using NuPage Novex 4%-12% Bis-Tris gels with MOPS running buffer (Invitrogen) and staining with Gelcode Blue reagent (Thermo Fisher Scientific). Western blotting was performed by separating 2.5 µg TeNT on a single gel and electroblotting to a nitrocellulose membrane. After blocking the membrane with PBS containing 5% milk and 0.05% Tween-20, immunoblotting was performed in PBS containing 0.1% milk and 0.05% Tween-20 using 0.5 µg/ml biotinylated VHHs and 0.1 µg/ml streptavidin-HRP conjugate. Blots were visualized for HRP by enhanced chemiluminescence (LI COR Biosciences, USA).

2.7. Epitope binning with biolayer interferometry

The Octet RED96 System (FortéBio-Sartorius, USA) was used to assess the binding of VHH monomers and multimers to independent TeNT antigenic sites. These in-tandem epitope binning assays were conducted in assay buffer consisting of PBS with 0.05% Tween 20 and 0.2% casein at 30 °C as follows. Streptavidin (SA)-sensors (FortéBio) were hydrated and loaded with biotinylated TeNT (5 µg/ml) for 11–17 min followed by incubation with blocking VHH multimers (100 nM) or assay buffer for 7–20 min and subsequent incubation with analyte VHH (15 nM) for 15–20 min. Three VHH multimers (T6T16A12, T6T15A12, T6T15G13) were each allowed to block TeNT coupled to sensors in fourfold and subsequently incubated with four analyte VHHs (T6L, T15L-3FW4M,

T16L or the same VHH multimer as the blocking VHH). The four analyte VHHs were also incubated on sensors loaded with TeNT only. For each analyte VHH the % inhibition of TeNT binding due to a blocking VHH multimer was then calculated as $100 - 100 \times [\text{association signal with blocking VHH}] / [\text{association signal without blocking VHH}]$.

2.8. Affinity measurements

The Octet RED96 and WAVEdelta technology (Creoptix® AG, Switzerland) were used. For both systems we used biotinylated TeNT as ligand and VHHs as analyte, and the reverse setup. The on-rate (k_a) and off-rate (k_d) were determined by global fitting of the association and dissociation phases of a series of analyte concentrations. The mathematical model used assumes a 1:1 stoichiometry, fitting only one analyte in solution binding to one binding site on the surface. The equilibrium dissociation constant (K_D), a measure for affinity, was then calculated as the ratio of k_d and k_a .

2.8.1. Octet RED96 experiments

Here we used the same (SA) sensors, assay buffer and assay temperature (30 °C) as described above and, in addition, a kinetics buffer (PBS, Fischer Scientific), with 0.02% Tween 20 (Acros Organics) and 0.2% casein (Thermo Scientific) in all experiments. The concentrations of TeNT and VHHs were optimized for affinity measurements prior to the experiments. The typical assay protocol was as follows: baseline for 60–300 sec, loading for 600–2300 sec, wash for 30 sec, association of serial dilutions of TeNT or VHHs for 120–600 sec and finally dissociation for 400–1800 sec. For data Analysis the v10.0 software (FortéBio) was used.

2.8.2. WAVEdelta experiments

The analyses were performed in running buffer (PBS with 0.02% Tween 20) with a flowrate between 10 and 60 µl/min, an injection duration between 60 and 300 sec and a dissociation duration between 45 and 6000 sec on the relevant channels, at 30 °C. In most cases, double referencing was used (control without ligand and control without analyte). The standard protocols were followed. In short, the polycarboxylate chip (WAVEchip 4PCP-S) was conditioned using running buffer. Biotinylated TeNT or VHHs were immobilized as ligand by streptavidin coupling (10 µl/min). One flow cell was treated the same way with only running buffer and used as a first reference (no ligand, no analyte). Before capturing the analyte, running buffer was passed over the flow cells as a second reference (ligand, no analyte) using the same protocol as the analyte. Subsequently, several serial dilutions of VHH or TeNT as analyte were sequentially passed over ligand-bound surface

(60 µl/min). Finally, running buffer was passed over the flow cells to wash off analyte bound to the ligand, thus allowing measurement of k_d . For data analysis the WAVE control software was used.

2.9. TeNT neutralization test

The test was based on the European Pharmacopoeia (Ph Eur) monograph 0091 for tetanus antitoxin. The toxin dose level in the assays performed was lowered to Lp/200 per mouse to allow a higher sensitivity of the assay. The samples were diluted such that the final starting concentration in the assay mixture (i.e. including toxin) was at a predefined concentration. Each dilution was mixed with a fixed amount of TeNT (toxin batch AWX4664, 1/100 dilution) and left to stand for 30 min prior to injection (0.5 ml s.c., left thigh). Each dilution group consisted of 4 mice, two-fold or four-fold serial dilutions were used. Animals were observed for 96 h for signs of tetanus paresis. In each of 3 assays (Study 1–3) a reference antitoxin (1st International Standard, Human Tetanus Immunoglobulin, TE3 / 26/488) was included in parallel to allow for calculation of the potency (IU/mg) of the VHH monomer or multimer (mixture) tested.

3. Results

3.1. Characterization of TeNT binding monomers

TeNT binding VHHs were selected from phage display libraries of at least 2×10^8 independent clones using both rTTC and TeNT that was either directly coated or immobilized with cAb-TT2 to permit the presentation of TeNT in multiple tertiary structure formats. After two rounds of panning individual VHHs clones were subjected to sequence analysis, resulting in a panel of 28 unique VHHs comprising 9 different CDR3 groups. In total 15 VHHs representing 7 different CDR3 groups were selected for production in yeast and further characterization (Fig. 1). VHHs were primarily selected based on the results in the ELISAs, a low predicted isoelectric point that correlates with high solubility and absence of deletions in conserved VHH framework regions. Furthermore, VHHs of two CDR3 groups were not selected because they contained 1 or 2 potential N-glycosylation sites close to the predicted antigen binding site which could thus potentially abrogate antigen binding. The ELISAs with biotinylated VHHs or mAbs on directly coated TeNT or TeNT immobilized using cAb-TT2 were overall consistent with ELISAs using their unlabeled counterparts (Fig. 1A, B), showing that biotinylation did not substantially affect antigen binding by VHHs or mAbs. TeNT, when immobilized with cAbTT2, captured all VHHs (Fig. 1A) and 12 VHHs also bound to directly coated TeNT (Fig. 1B) and rTTC (Fig. 1C). In total 12 VHHs partially inhibited TeNT-GT1b interaction. The 3 CDR3 group B VHHs inhibited TeNT-GT1b interaction less effectively when compared to CDR3 group A, C and D VHHs as revealed by a 2.4- to 25-fold lower $1/IC_{50}$ value of the CDR3 group B VHHs (Fig. 1D). T5L is the only rTTC binding VHH that does not inhibit TeNT-GT1b interaction. A synergistic effect towards TeNT-GT1b inhibition due to mixing of VHHs was not observed (Table S2). An ELISA with captured TTC again confirmed that T2L and T3L do not bind to rTTC (Table S3). VHH T3L bound to TeNT immobilized with mAb TT10 (data not shown). Only mAbs 6E7 and 6F57 out of 5 TeNT neutralizing mAbs analysed (Table S1), bound to rTTC (Fig. 1C).

3.2. Epitope binning with TeNT binding monomers

To enable the design of multimers that bind to different epitopes on antigenic subdomains of a single TeNT molecule, epitope binning was performed.

In total 10 VHHs and 6 mAbs were selected for epitope binning by ELISA (Table 2). We used at most 2 VHH representatives from each CDR3 group since VHHs from the same CDR3 group most likely originate from the same B-cell clone and therefore recognize the same antigenic site. We omitted T5L since it was poorly produced. All VHHs and mAbs blocked the binding of their biotinylated counterpart by at least 75%, indicating that the assay was valid. The VHHs fall into five independent antigenic sites that we indicated by roman numerals I to V. As expected, VHHs from the same CDR3 group are always part of the same antigenic site. Antigenic site V is detected by four VHHs from 2 CDR3 groups. The VHH T2L, mAb 14F5 and 6F55 recognize antigenic site I. Antigenic site IV (T6L and T8L) could represent a linear epitope as demonstrated by Western blot (Fig. S1).

3.3. Production and characterization of bispecific VHH multimers

Multimers were designed that combined two characteristics - they had to possess high affinity to TeNT and promote serum longevity.

The details of 11 VHH multimers (8 VHH dimers (VHH2s) and 3 VHH trimers (VHH3s)) are provided in Table 1. Four TeNT-binding VHHs (T2, T6, T15-3FW4M, T16) were selected because they recognize four separate antigenic sites and either blocked GT1b receptor interaction (T6, T15-3FW4M and T16) or competed in ELISA with TeNT neutralizing mAbs (T2 and T6; Table 2).

Production of these VHH multimers without a myc tag yielded single molecules of the expected molecular weight, approximately 30 kD for a VHH2 and 45 kD for a VHH3 (Fig. 2). The VHH monomers which contained a myc tag yielded an additional molecule with an approximately 2-kDa higher molecular mass which presumably represents partial O-glycosylation related to the presence of the tag as reported [48].

The production level of the VHH multimers ranged from 1 to 99 mg/l (Table 1). TeNT binding of VHH multimers was analyzed by three different ELISAs (Fig. 3). The binding of multimers to directly coated TeNT, except for T2- containing VHH2s, confirmed the properties found for the respective monomers. The $1/EC$ values are often slightly higher as compared to the VHH monomers, presumably due to better recognition of multimers by the anti-llama polyclonal used. In an ELISA using coated IgG or Alb, and biotinylated TeNT for detection, all multimers showed bispecific binding to both TeNT and IgG or Alb. All monomers were negative in this ELISA. The VHH multimers demonstrated IC_{50} values in the GT1b-TeNT inhibition ELISA that were comparable to their monomer counterparts.

The in-tandem blocking assays (Fig. 4) demonstrated that the VHH3s could fully block the binding of the same VHH3 as well as the 2 VHH monomers that are also represented in the VHH3s, confirming the correct composition of the VHH3s. All three VHH3s also block binding of a third TTC-binding VHH monomer that is not represented in the VHH3. Such blocking is partial in the case of T16L that is not represented in T6T15A12 (40%) nor in T15T6G13 (30%), whereas 100% blocking of T15L-3FW4M occurs by T6T16A12 which lacks T15 (Fig. 4).

3.4. Monomer and multimer VHHs affinity for TeNT

The results are shown in Table 3 and supplemental Fig. S2. The monomers T2L, T6L, T15L and T16L all had affinities in the range of 0.2–0.9 nM. The VHH T3L had a very high affinity of 1.4 pM. The VHH3 multimers T6T16A12, T6T15A12 and T6T15G13 had a K_D of 4–23 pM. Affinity measurements varied between the different ligand-analyte setups by a factor of, at most, five-fold. This could be due to variabilities in biotinylation of the ligand interfering with binding of the analyte or variability in VHH or TeNT concentration

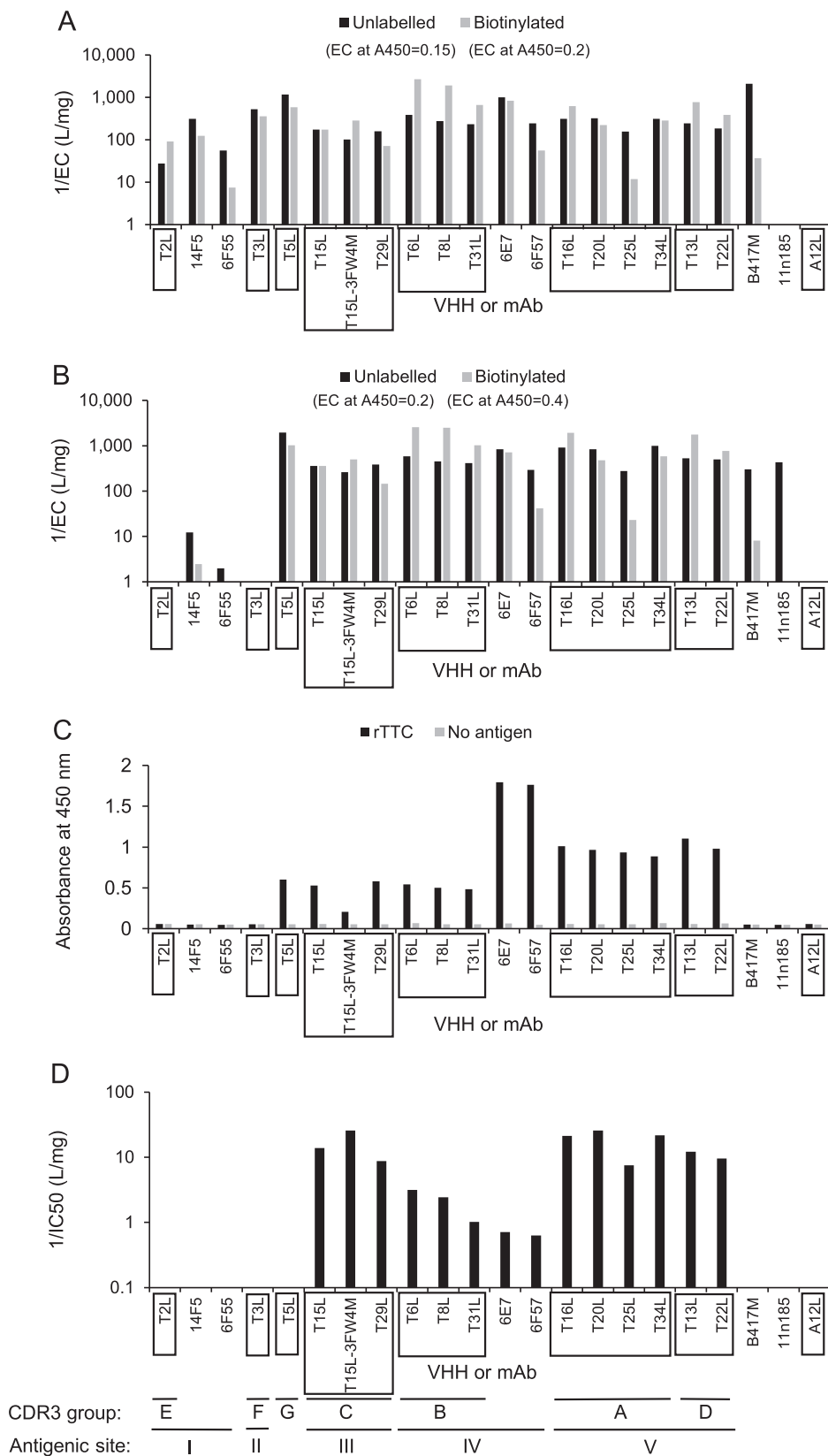


Fig. 1. TeNT binding of VHHs and mAbs in different ELISA setups. Binding of unlabeled or biotinylated VHH or mAb to either cAb-TT2 immobilized TeNT (A) or coated TeNT (B) is shown. Panel C shows the absorbance value of a single VHH or mAb at a single concentration when bound to coated rTTC or the corresponding negative control (no antigen). Panel D shows inhibition of TeNT- ganglioside interaction by VHHs or mAbs in ELISA. In panels A, B and D dilution series of VHHs or mAbs were incubated. The reciprocal of the EC value (A and B) or the IC50 value (D) is presented. The EC values were interpolated at the A450 values indicated in the legends of panels A and B. VHHs belonging to the same CDR3 group are boxed while mAbs are not boxed. The letters to identify a CDR3 group (A-G) or independent antigenic site (I-V) are indicated at the bottom.

Table 2
Epitope binning of TeNT binding VHHs and mAbs by competition ELISA.

VHH or mAb ^b	CDR3 Group	Inhibition of binding of biotinylated VHH or mAb (%) ^a																Antigenic site	TTC binding ^c
		T2L	14F5	6F55	T3L	T15L	T15L-3FW4M	T6L	T8L	6E7	6F57	T13L	T22L	T16L	T34L	B417M	11n185		
T2L	E	96	97	94	9	6	12	2	16	8	19	21	3	26	-16	-11	19	I	-
14F5	-	81	78	54	28	6	16	12	22	-16	9	42	-28	0	20	35	14	I	-
6F55	-	72	85	78	10	4	41	16	30	29	-24	39	10	17	12	33	27	I	-
T3L	F	10	-8	35	97	12	10	10	10	-12	17	23	10	18	-4	0	-26	II	-
T15L	C	6	7	-2	-5	96	96	1	15	6	4	2	2	5	10	5	0	III	+
T15L-3FW4M	C	10	2	-4	-8	96	95	7	6	6	6	-5	4	3	3	-9	-1	III	+
T6L	B	11	11	4	-3	14	12	96	97	67	53	7	3	-3	11	4	5	IV	+
T8L	B	7	3	1	0	6	12	95	96	66	50	5	6	8	8	0	4	IV	+
6E7	-	12	8	1	4	4	7	18	35	75	64	-3	1	-2	7	0	6	IV	+
6F57	-	4	3	-1	-3	-1	10	45	49	88	85	-4	7	0	11	1	-3	IV	+
T13L	D	7	5	1	1	-19	8	1	13	2	0	95	92	91	91	4	2	V	+
T22L	D	4	0	-2	5	2	11	6	1	8	10	95	94	92	93	-2	3	V	+
T16L	A	13	6	-3	-1	12	17	-8	2	6	2	96	96	95	95	-1	-2	V	+
T34L	A	2	4	-3	0	3	14	-2	-4	10	13	93	94	93	95	-2	2	V	+
B417M	-	-220	-23	-44	7	66	-33	11	-56	66	65	6	66	-56	-43	79	-146	-	-
11n185	-	-43	-24	-17	19	18	3	5	-4	19	16	1	38	-14	-11	15	84	-	-

^aValues above or equal to 50 are indicated in grey background color. mAb names are underlined.

^bBiotinylated VHH or mAb is in rows and unlabeled VHH or mAb in columns.

^c- , no TTC binding; + , TTC binding. Based on Fig. 1C.

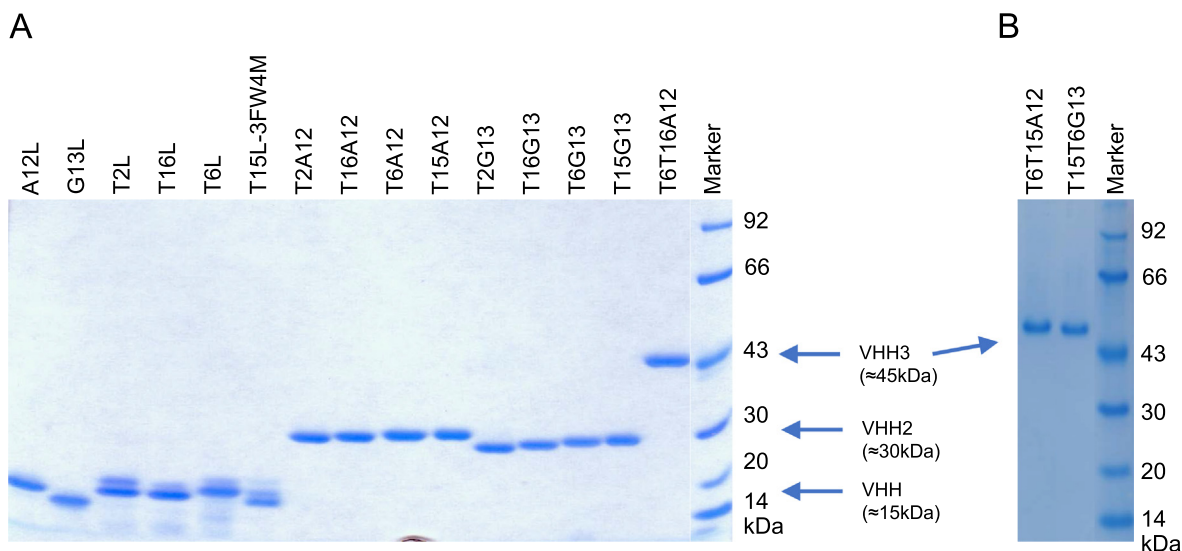


Fig. 2. SDS PAGE analysis of VHH monomers, dimers (VHH2s) and trimers (VHH3s) produced in yeast. Panels (A) and (B) represent two different gels. The position of VHHs, VHH2s or VHH3s is indicated by arrows. The molecular weights of the marker proteins are indicated at the right.

determination. It is not unusual to observe differences in affinities between different measurement techniques [15].

3.5. TeNT neutralizing in vivo potency

Three consecutive studies were performed (Table 4). The International Standard for Tetanus Antitoxin (TE-3) performed as expected in all 3 studies with similar end points of 0.0325 IU, 0.0325 IU and 0.034 IU, respectively.

We preferentially used VHH multimers for this assay, since these have the potential to provide *in vivo* serum half-life extension. However, monomer T3L was also included since this VHH covers a separate antigenic site and possesses very high affinity. Study 1 showed that two out of four VHH2s did not neutralize TeNT at a concentration of 1000 nM. The two VHH2s with either

T6 or T15-3FW4M had a potency between 1.0 and 1.2 IU per mg. The VHH3 T6T16A12, showed complete protection at the lowest concentration analyzed (3.1 nM). In study 2 T6T16A12 again showed complete protection at the lowest concentration analyzed (0.2 nM). The combinations T6G13 + T16G13 or T6G13 + T15G13 showed full protection at the lowest concentration analyzed (3.91 nM). An additional synergistic effect of T2G13 or T3L present in the mixtures of four VHHs could thus not be demonstrated. The combination of T15G13 with T16G13 (total concentration 125 nM) was not protective. In study 3, T6T16A12 was further titrated which finally resulted in an endpoint of neutralization that allowed estimation of its potency to be 1510 IU/mg. The two VHHs T6G13 and T16G13 when tested at lower dilutions let to an endpoint estimate of full protection between 0.4 and 3.91 nM. Since the individual T6G13 VHH showed full protection at 1000 nM and T16G13 did

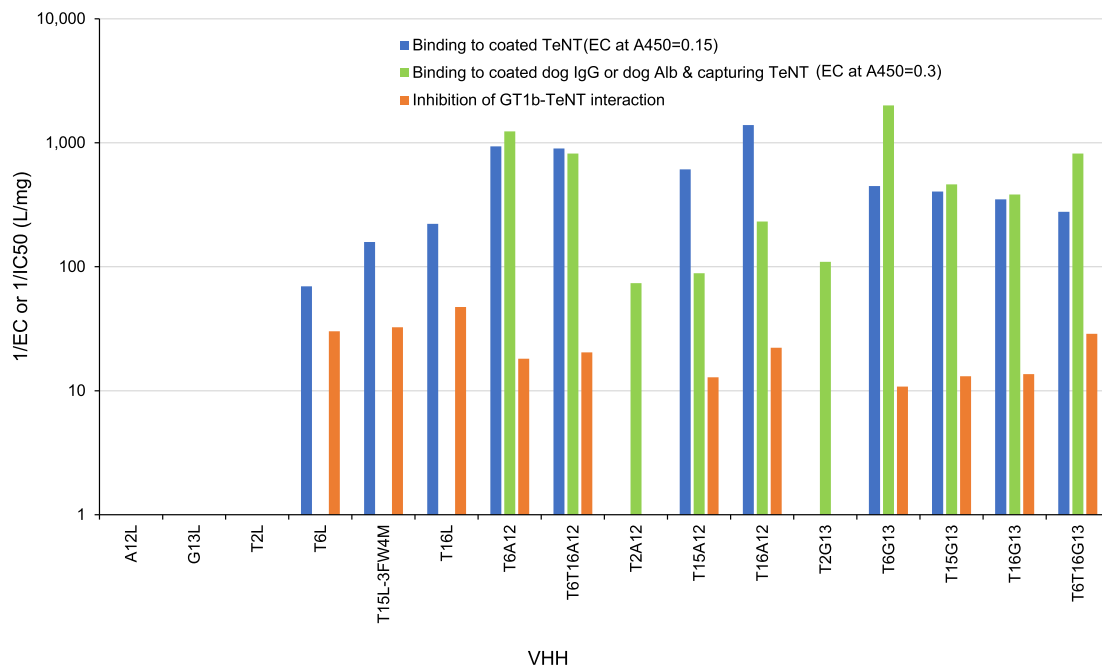


Fig. 3. The binding in ELISA of multimer VHHs to TeNT both monospecific and bispecific in combination with dog IgG or albumin. Monospecific VHH binding to TeNT was analyzed both by TeNT – ganglioside inhibition ELISA and on plates coated with TeNT. In addition, bispecific binding requiring VHH binding to coated dog albumin (A12 containing multimeric VHHs) or dog IgG (G13 containing multimeric VHHs) and capture of soluble biotinylated TeNT is shown. The reciprocal of the EC or IC value of each VHH is shown. The EC values were interpolated at the indicated A450 values.

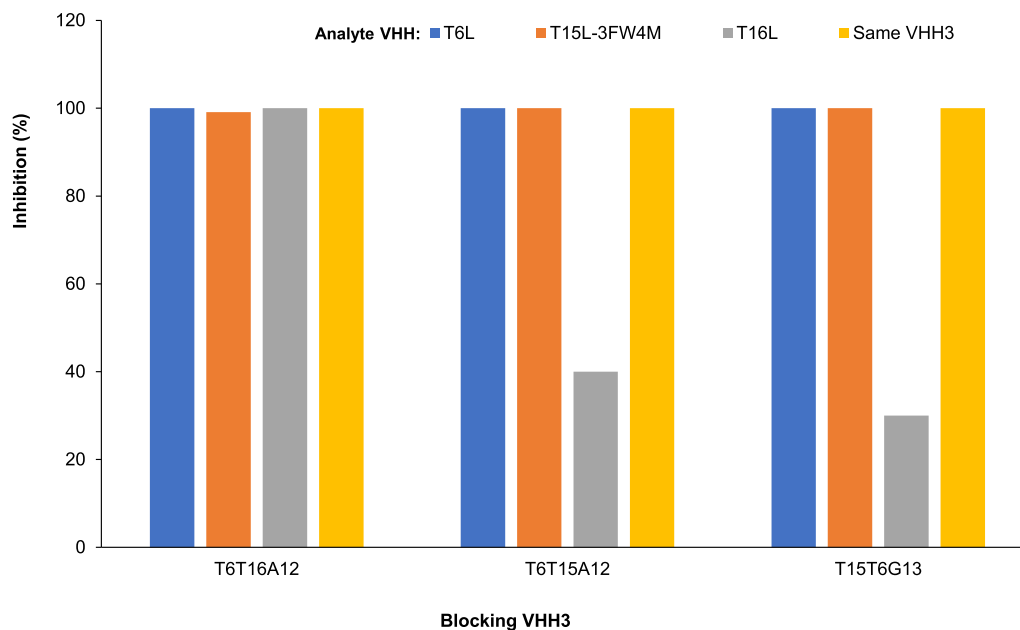


Fig. 4. Blocking by VHH3s of TeNT binding of 3 monomeric VHHs or the same VHH3 that was used for blocking. In biolayer interferometry experiments sensors were loaded with biotinylated TeNT and subsequently with blocking VHH3s. Then sensors were loaded with monomeric analyte VHHs or the same VHH3 as used for blocking. The percentage inhibition of the association signal of analyte VHHs as compared to a control assay without prior blocking by VHH3s is given.

not protect at 1000 nM, the level of synergy obtained with T6T16A12 is at least 250–1000-fold. The mixture of T15G13 and T6T16A12 was almost equally as potent as T6T16A12 alone.

4. Discussion

In total, 11 VHHs were isolated that inhibited TeNT- ganglioside interaction, bound TTC in ELISA and covered 3 epitope bins. For

in vivo evaluation of TeNT neutralization, we selected 3 VHHs (T6, T15 and T16) covering all 3 bins on TTC and VHHs T2 and T3 addressing two other bins. VHH2s were generated by fusion to an albumin or immunoglobulin binding VHH domain. The VHH2s containing T6 and T15 show *in vivo* neutralization at a concentration of 1000 nM or 500 nM, respectively, whereas T16 did not. The observation that VHHs that inhibit TeNT-ganglioside interaction, such as T16, do not neutralize TeNT *in vivo* has been reported [15,50,51]. Mixtures of VHH2s containing T6 and T16 or T6 and

Table 3
TeNT binding affinity/avidity of VHH monomers and multimers when evaluated with two different technologies.

VHHs	Analyte:	Octet Red96						Creoptix WAVEdelta					
		K _D (pM)		k _d (1/s) (10 ⁻⁷)		Dissociation Interval (sec)		K _D (pM)		k _d (1/s) (10 ⁻⁷)		Dissociation Interval (sec)	
		VHH	TeNT	VHH	TeNT	VHH	TeNT	VHH	TeNT	VHH	TeNT	VHH	TeNT
T2L		656	ND ^a	2800	ND	750	ND	ND	ND	ND	ND	ND	ND
T3L		<10 ^b	ND	<100 ^b	ND	1800	ND	1.4	ND	66	ND	6000	ND
T6L		224	535	1134	627	1800	1800	ND	ND	ND	ND	ND	ND
T15L		413	772	387	857	750	1800	ND	ND	ND	ND	ND	ND
T16L		339	932	3110	870	400	1800	ND	ND	ND	ND	ND	ND
T6T16A12		13	11	132	44	400	1800	8.9	7.2	101	22	6000	6000
T6T15A12		<10	<10	<100	<100	400	1000	17	3.8	100	15	12,000	6000
T15T6G13		<10	<10	<100	<100	400	1000	23	7.4	273	23	6000	6000

^a ND, not determined.

^b K_D or k_d was not calculated because there was no measurable dissociation within the time interval used.

Table 4
In vivo protection against tetanus toxin challenge in 3 studies.

VHH/VHH combination	VHH in 1st dilution ^a (nM)	Lowest VHH concentration giving 100% protection (nM)	Potency (IU/mg)
<i>Study 1</i>			
T2G13	1000	>1000	<1.04
T3L	1000	>1000	<1.04
T6G13	1000	1000	1.04
T15G13	1000	500	1.21
T16G13	1000	>1000	<1.04
T6T16A12	100	≤3.1	>93
<i>Study 2</i>			
T6G13 + T16G13	125	≤3.91 ^b	ND ^c
T2G13 + T3L + T6G13 + T16G13	125	≤3.91	ND
T6G13 + T15G13	125	≤3.91	ND
T2G13 + T3L + T6G13 + T15G13	125	≤3.91	ND
T15G13 + T16G13	125	>125	ND
T15G13 + T6T16A12	68.75	≤2.15	ND
T6T16A12	6.25	≤0.2	>1478
<i>Study 3^d</i>			
T6T16A12	0.2	0.2 ^e	1510
T6G13 + T16G13	0.4	> 0.4	ND
T15G13 + T6T16A12	0.4	0.4	ND

^a For VHH mixtures the total VHH concentration is given; i.e. the individual VHHs are present at equivalent (molar) amounts.

^b Full protection at all dilutions.

^c ND, not determined since it contains mixture of VHHs.

^d Fourfold dilution steps; in other two studies a twofold dilution step was used.

^e 50% protection at top dilution only.

T15, but not T16 and T15, lead to strong (more than 100-fold) synergistic protection *in vivo*.

Increased potency of multimer VHHs when they recognize independent antigenic sites has been reported [14,24,33,34,52]. We constructed VHH3s composed of both T6 and T15 or T6 and T16 to augment receptor blocking properties. The *in vivo* potency of T6T16A12 (Fig. S3) was between 2 and 20-fold higher than that of the mixture of T6G13 and T16G13. The higher affinity of the multimer (K_D 7–13 pM) as compared to the corresponding constituent VHH monomers (K_D 224–932 pM) is likely of significance. In addition, epitope binning showed that T6T16A12 also blocked binding of T15 monomers. VHH T15 recognizes a unique domain and as VHH2 neutralizes TeNT. The orientation of T6T16A12 when bound to TeNT, or the presence of either linkers or the A12 VHH increases the covered surface area likely encompassing the 2 ganglioside binding sites [21,22]. However, other mechanisms can also explain the increased potency of T6T16A12 such as TeNT aggregation, similar to antibody neutralization of other toxins [33,53–55],

or conformational changes [56] due to binding [15,25]. Elucidation of the exact binding sites of the monomers would support the rational design of additional VHH multimers covering multiple (functional) domains, as recently shown for BoNT [57].

A strength of the current approach was the isolation of a set of VHHs that enabled a rational design of multimers. Here, the coated (TeNT and rTTC) or indirect presentation of TeNT in various test setups was important as was noted for selection of diphtheria toxin neutralizing mAbs [17], but which was often neglected while isolating TeNT binding (recombinant) antibodies [10,11,13,25,28,50,51], although not always [15]. In an earlier study, three VHHs were obtained that inhibited rTTC binding to GT1b gangliosides and bound to rTTC with moderate affinity (K_D = 1.5–5.0 nM), but did not yield VHH multimers showing increased *in vivo* TeNT neutralization [50]. Mixtures of 3 mAbs can provide better protection than mixtures of 2 mAbs against both TeNT [10] and BoNT [32]. Multimers composed of 4 VHH domains have been described [36,58,59] thus inclusion of a third TeNT binding VHH (e.g. T2 or T3) into T6T16A12 is possible. It would add another functional domain which in a VHH4 format could restrict the necessary conformations that TeNT assumes after entering neurons [20]. Especially T3L, with its extreme high affinity could be of interest. Of course searching for novel VHHs that cover more of the 20 competition bins already identified can also lead to potent multimers [10]. In a similar approach for ricin toxin, a panel of 68 unique VHHs covering 20 competition bins [52] offers multiple design options for multimers.

T6T16A12 neutralized TeNT in a standardized mouse bioassay at 1510 IU/mg, which compares favorably to commercial human immunoglobulin antitoxin preparations which have potencies of 1–2.5 IU/mg, and to a potency of 29.5 IU/mg of the horse immunoglobulin antitoxin TE 6/66/2 [60], and mixtures of 2 or more mAbs with potencies of 15–77 IU/mg [10]. A human mAb mixture provided protection at an amount of 0.625 µg (equating to 4.2 nM) [13] which is less than the VHH2 mixtures evaluated in this study. The administration of the recommended dose of 500–1000 IU/kg equine antitoxin in established human cases of tetanus [61] requires a dose of 0.5 mg/kg of T6T16A12. A similar dose regime (100–1000 IU/kg) is recommended for cats and dogs [62].

The serum half-life of T6T16A12 was successfully extended in two different species [45]. However, the A12 VHH in T6T16A12 does not bind to albumin of mice [45], thus it is highly potent without serum half-life extension in mice. This is not surprising considering the experimental setup where toxin is pre-mixed with VHH prior to injection, which can also confer protection with monovalent VHHs [50]. The ability of T6T16A12 to bind serum albumin *in vivo* when administered to the target species (e.g. horse) could

further enhance its potency either due to the increased serum half-life, as suggested for an anti-TeNT VHH fused to an anti-CD11 VHH [50], or through increased steric hindrance. Similarly, improved *in vivo* potency of a recombinant antibody due to complexing with IgG has been observed [14,63,64].

The gene coding for TeNT is highly conserved among isolates of *C. tetani* [65], thus billions of tetanus toxoid vaccine dosages have been used without reports of lack of efficacy due to antigen divergence [66]. Hence, enhanced cross-reactivity to antigenic variants by VHH multimers [36] is in the case of TeNT of minor clinical interest. Even more so, if a single mutation in this gene would occur it is unlikely that the (bivalent) binding of T6T16A12 would be abolished. The favorable characteristics of the novel VHH trimer T6T16A12 warrant further development for medical use [67] such as to provide a better product profile than existing serum derived products [1,27].

CRedit authorship contribution statement

Hans Smit: Conceptualization, Formal analysis, Writing - review & editing, Writing - original draft, Funding acquisition. **Bart Ackerschott:** Data curation, Formal analysis, Writing - review & editing. **Robert Tierney:** Data curation, Formal analysis, Writing - review & editing. **Paul Stickings:** Formal analysis, Writing - review & editing. **Michiel M. Harmsen:** Conceptualization, Data curation, Formal analysis, Writing - review & editing.

Declaration of Competing Interest

The authors declare the following financial interests/personal relationships which may be considered as potential competing interests: The work described was sponsored by Smivet B.V., Wijchen, The Netherlands. B. Ackerschott and H. de Smit were employed by Smivet B.V.

Acknowledgements

Conny van Solt, Sandra van de Water and Marga van Setten (Wageningen Bioveterinary Research) for technical assistance in llama immunization, phage display selections and VHH production in yeast, respectively.

Appendix A. Supplementary data

Supplementary data to this article can be found online at <https://doi.org/10.1016/j.jvax.2021.100099>.

References

- Yen LM, Thwaites CL. Tetanus. *Lancet* 2019;393:1657–68. [https://doi.org/10.1016/S0140-6736\(18\)33131-3](https://doi.org/10.1016/S0140-6736(18)33131-3).
- van Galen G, Rijckaert J, Mair T, Amory H, Armengou L, Bezdekova B, et al. Retrospective evaluation of 155 adult equids and 21 foals with tetanus from Western, Northern, and Central Europe (2000–2014). Part 2: Prognostic assessment. *J Vet Emerg Crit Care (San Antonio)*. 2017;27:697–706. <https://doi.org/10.1111/vec.12669>.
- Adamantos S, Boag A. Thirteen cases of tetanus in dogs. *Vet Rec* 2007;161:298–302. <https://doi.org/10.1136/vr.161.9.298>.
- Maksimovic A, Filipovic S, Lutvikadic I, Šunje-Rizvan A. Tetanus in cat: from neglected wound to neuromuscular disorder—case report. *J Life Sci* 2016;10:182–4. <https://doi.org/10.17265/1934-7391/2016.04.002>.
- Von Behring E, Kitasato S. Ueber das zustandekommen der Diphtherie-immunität und der tetanus-immunität bei Thieren. *Dtsch Med Wochenschr*. 1890;16:1113–4.
- Kaufmann SH. Remembering Emil von Behring: from Tetanus Treatment to Antibody Cooperation with Phagocytes. *mBio*. 2017;8. <https://doi.org/10.1128/mBio.00117-17>.
- Postel A, Cavalleri JM, Pfaender S, Walter S, Steinmann E, Fischer N, et al. Frequent presence of hepaci and pegiviruses in commercial equine serum pools. *Vet Microbiol* 2016;182:8–14. <https://doi.org/10.1016/j.vetmic.2015.10.032>.
- Divers TJ, Tennant BC, Kumar A, McDonough S, Cullen J, Bhuvu N, et al. New parvovirus associated with serum hepatitis in horses after inoculation of common biological product. *Emerg Infect Dis* 2018;24:303–10. <https://doi.org/10.3201/eid2402.171031>.
- Arbabi-Ghahroudi M. Camelid single-domain antibodies: historical perspective and future outlook. *Front Immunol* 2017;8:1589. <https://doi.org/10.3389/fimmu.2017.01589>.
- Volk WA, Bizzini B, Snyder RM, Bernhard E, Wagner RR. Neutralization of tetanus toxin by distinct monoclonal antibodies binding to multiple epitopes on the toxin molecule. *Infect Immun*. 1984;45:604–9.
- Lang AB, Cryz Jr SJ, Schurch U, Ganss MT, Bruderer U. Immunotherapy with human monoclonal antibodies. Fragment A specificity of polyclonal and monoclonal antibodies is crucial for full protection against tetanus toxin. *J Immunol* 1993;151:466–72.
- Arbabi-Ghahroudi M, Desmyter A, Wyns L, Hamers R, Muylderms S. Selection and identification of single domain antibody fragments from camel heavy-chain antibodies. *FEBS Lett* 1997;414:521–6.
- Aliprandini E, Takata DY, Lepique A, Kalil J, Boscardin SB, Moro AM. An oligoclonal combination of human monoclonal antibodies able to neutralize tetanus toxin *in vivo*. *Toxicon* 2019;X2:100006. <https://doi.org/10.1016/j.tox.2019.100006>.
- Mukherjee J, Tremblay JM, Leysath CE, Ofori K, Baldwin K, Feng X, et al. A novel strategy for development of recombinant antitoxin therapeutics tested in a mouse botulism model. *PLoS ONE* 2012;7:e29941. <https://doi.org/10.1371/journal.pone.0029941>.
- Scott N, Qazi O, Wright MJ, Fairweather NF, Deonarain MP. Characterisation of a panel of anti-tetanus toxin single-chain Fvs reveals cooperative binding. *Mol Immunol* 2010;47:1931–41. <https://doi.org/10.1016/j.molimm.2010.02.020>.
- Wang H, Yu R, Fang T, Yu T, Chi X, Zhang X, et al. Tetanus neurotoxin neutralizing antibodies screened from a human immune scFv antibody phage display library. *Toxins* 2016;8. <https://doi.org/10.3390/toxins8090266>.
- Wenzel EV, Bosnak M, Tierney R, Schubert M, Brown J, Dubel S, et al. Human antibodies neutralizing diphtheria toxin *in vitro* and *in vivo*. *Sci Rep* 2020;10:571. <https://doi.org/10.1038/s41598-019-57103-5>.
- Emsley P, Fotinou C, Black I, Fairweather NF, Charles IG, Watts C, et al. The structures of the H(C) fragment of tetanus toxin with carbohydrate subunit complexes provide insight into ganglioside binding. *J Biol Chem* 2000;275:8889–94.
- Fotinou C, Emsley P, Black I, Ando H, Ishida H, Kiso M, et al. The crystal structure of tetanus toxin Hc fragment complexed with a synthetic GT1b analogue suggests cross-linking between ganglioside receptors and the toxin. *J Biol Chem* 2001;276:32274–81. <https://doi.org/10.1074/jbc.M103285200>.
- Masuyer G, Conrad J, Stenmark P. The structure of the tetanus toxin reveals pH-mediated domain dynamics. *EMBO Rep* 2017;18:1306–17. <https://doi.org/10.15252/embr.201744198>.
- Rummel A, Bade S, Alves J, Bigalke H, Binz T. Two carbohydrate binding sites in the H(CC)-domain of tetanus neurotoxin are required for toxicity. *J Mol Biol* 2003;326:835–47. [https://doi.org/10.1016/S0022-2836\(02\)01403-1](https://doi.org/10.1016/S0022-2836(02)01403-1).
- Chen C, Fu Z, Kim JJ, Barbieri JT, Baldwin MR. Gangliosides as high affinity receptors for tetanus neurotoxin. *J Biol Chem* 2009;284:26569–77. <https://doi.org/10.1074/jbc.M109.027391>.
- Schiavo G, Benfenati F, Poulain B, Rossetto O, Polverino de Lauro P, DasGupta BR, et al. Tetanus and botulinum-B neurotoxins block neurotransmitter release by proteolytic cleavage of synaptobrevin. *Nature* 1992;359:832–5. <https://doi.org/10.1038/359832a0>.
- Kuhn P, Fuhner V, Unkauf T, Moreira GM, Frenzel A, Miethe S, et al. Recombinant antibodies for diagnostics and therapy against pathogens and toxins generated by phage display. *Proteomics Clin Appl* 2016;10:922–48. <https://doi.org/10.1002/prca.201600002>.
- Fitzsimmons SP, Clark KC, Wilkerson R, Shapiro MA. Inhibition of tetanus toxin fragment C binding to ganglioside G(T1b) by monoclonal antibodies recognizing different epitopes. *Vaccine* 2001;19:114–21. [https://doi.org/10.1016/S0264-410X\(00\)00115-8](https://doi.org/10.1016/S0264-410X(00)00115-8).
- Halpern JL, Loftus A. Characterization of the receptor-binding domain of tetanus toxin. *J Biol Chem* 1993;268:11188–92.
- Lukic I, Marinkovic E, Filipovic A, Krnjaja O, Kosanovic D, Inic-Kanada A, et al. Key protection factors against tetanus: Anti-tetanus toxin antibody affinity and its ability to prevent tetanus toxin - ganglioside interaction. *Toxicon* 2015;103:135–44. <https://doi.org/10.1016/j.toxicon.2015.06.025>.
- Sheppard AJ, Cussell D, Hughes M. Production and characterization of monoclonal antibodies to tetanus toxin. *Infect Immun* 1984;43:710–4.
- Williamson LC, Bateman KE, Clifford JC, Neale EA. Neuronal sensitivity to tetanus toxin requires gangliosides. *J Biol Chem* 1999;274:25173–80. <https://doi.org/10.1074/jbc.274.35.25173>.
- Luo P, Qin L, Mao X, Chen L, Yu S, Li Q, et al. Identification of a novel linear epitope in tetanus toxin recognized by a protective monoclonal antibody: implications for vaccine design. *Vaccine* 2012;30:6449–55. <https://doi.org/10.1016/j.vaccine.2012.08.002>.
- Kakita M, Takahashi T, Komiya T, Iba Y, Tsuji T, Kurosawa Y, et al. Isolation of a human monoclonal antibody with strong neutralizing activity against diphtheria toxin. *Infect Immun* 2006;74:3682–3. <https://doi.org/10.1128/IAI.01731-05>.
- Nowakowski A, Wang C, Powers DB, Amersdorfer P, Smith TJ, Montgomery VA, et al. Potent neutralization of botulinum neurotoxin by recombinant

- oligoclonal antibody. *Proc Natl Acad Sci USA* 2002;99:11346–50. <https://doi.org/10.1073/pnas.172229899>.
- [33] Herrera C, Tremblay JM, Shoemaker CB, Mantis NJ. Mechanisms of ricin toxin neutralization revealed through engineered homodimeric and heterodimeric camelid antibodies. *J Biol Chem* 2015. <https://doi.org/10.1074/jbc.M115.658070>.
- [34] Moayeri M, Leysath CE, Tremblay JM, Vrentas C, Crown D, Leppla SH, et al. A heterodimer of a VHH (variable domains of camelid heavy chain-only) antibody that inhibits anthrax toxin cell binding linked to a VHH antibody that blocks oligomer formation is highly protective in an anthrax spore challenge model. *J Biol Chem* 2015;290:6584–95. <https://doi.org/10.1074/jbc.M114.627943>.
- [35] De Vlieger D, Ballegeer M, Rossey I, Schepens B, Saelens X. Single-domain antibodies and their formatting to combat viral infections. *Antibodies (Basel)* 2018;8. <https://doi.org/10.3390/antib8010001>.
- [36] Laursen NS, Friesen RHE, Zhu X, Jongeneelen M, Blokland S, Vermond J, et al. Universal protection against influenza infection by a multidomain antibody to influenza hemagglutinin. *Science* 2018;362:598–602. <https://doi.org/10.1126/science.aag0620>.
- [37] Harmsen MM, Van Solt CB, Fijten HPD, Van Setten MC. Prolonged *in vivo* residence times of llama single-domain antibody fragments in pigs by binding to porcine immunoglobulins. *Vaccine* 2005;23:4926–34. <https://doi.org/10.1016/j.vaccine.2005.05.017>.
- [38] Hoefman S, Ottevaere I, Baumeister J, Sargentini-Maier M. Pre-clinical intravenous serum pharmacokinetics of albumin binding and non-half-life extended nanobodies®. *Antibodies*. 2015;4:141–56. <https://doi.org/10.3390/antib4030141>.
- [39] Coombes L, Tierney R, Rigsby P, Sesardic D, Stickings P. In vitro antigen ELISA for quality control of tetanus vaccines. *Biologicals* 2012;40:466–72. <https://doi.org/10.1016/j.biologicals.2012.07.011>.
- [40] Harmsen MM, Fijten HPD. Improved functional immobilization of llama single-domain antibody fragments to polystyrene surfaces using small peptides. *J Immunoassay Immunochem* 2012;33:234–51. <https://doi.org/10.1080/15321819.2011.634473>.
- [41] Harmsen MM, Blokker JC, Pritz-Verschuren SB, Bartelink W, Van der Burg H, Koch G. Isolation of panels of llama single-domain antibody fragments binding all nine neuraminidase subtypes of influenza A virus. *Antibodies* 2013;2:168–92. <https://doi.org/10.3390/antib2020168>.
- [42] Russo G, Meier D, Helmsing S, Wenzel E, Oberle F, Frenzel A, et al. Parallelized antibody selection in microtiter plates. *Methods Mol Biol* 2018;1701:273–84. https://doi.org/10.1007/978-1-4939-7447-4_14.
- [43] Harmsen MM, Seago J, Perez E, Charleston B, Eble PL, Dekker A. Isolation of single-domain antibody fragments that preferentially detect intact (146S) particles of foot-and-mouth disease virus for use in vaccine quality control. *Front Immunol* 2017;8:960. <https://doi.org/10.3389/fimmu.2017.00960>.
- [44] Lefranc MP, Pommie C, Ruiz M, Giudicelli V, Foulquier E, Truong L, et al. IMGT unique numbering for immunoglobulin and T cell receptor variable domains and Ig superfamily V-like domains. *Dev Comp Immunol* 2003;27:55–77. [https://doi.org/10.1016/S0145-305X\(02\)00039-3](https://doi.org/10.1016/S0145-305X(02)00039-3).
- [45] De Smit AJ, Harmsen MM. Single domain antibodies binding to tetanus neurotoxin. International patent application WO 2019/175250; 2019.
- [46] Harmsen MM, van Solt CB, Hoogendoorn A, van Zijderveld FG, Niewold TA, van der Meulen J. *Escherichia coli* F4 fimbriae specific llama single-domain antibody fragments effectively inhibit bacterial adhesion in vitro but poorly protect against diarrhoea. *Vet Microbiol* 2005;111:89–98. <https://doi.org/10.1016/j.vetmic.2005.09.005>.
- [47] Huston JS, Levinson D, Mudgett-Hunter M, Tai MS, Novotny J, Margolies MN, et al. Protein engineering of antibody binding sites: recovery of specific activity in an anti-digoxin single-chain Fv analogue produced in *Escherichia coli*. *Proc Natl Acad Sci* 1988;85:5879–83.
- [48] Harmsen MM, Fijten HPD, Dekker A, Eblé PL. Passive immunization of pigs with bispecific llama single-domain antibody fragments against foot-and-mouth disease and porcine immunoglobulin. *Vet Microbiol* 2008;132:56–64. <https://doi.org/10.1016/j.vetmic.2008.04.030>.
- [49] Gorlani A, Lutje Hulsik D, Adams H, Vriend G, Hermans P, Verrips T. Antibody engineering reveals the important role of J segments in the production efficiency of llama single-domain antibodies in *Saccharomyces cerevisiae*. *Protein Eng Des Sel* 2012;25:39–46. <https://doi.org/10.1093/protein/gzr057>.
- [50] Rossotti MA, Gonzalez-Techera A, Guarnaschelli J, Yim L, Camacho X, Fernandez M, et al. Increasing the potency of neutralizing single-domain antibodies by functionalization with a CD11b/CD18 binding domain. *mAbs*. 2015;7:820–8. <https://doi.org/10.1080/19420862.2015.1068491>.
- [51] Yousefi M, Khosravi-Eghbal R, Reza Mahmoudi A, Jeddi-Tehrani M, Rabbani H, Shokri F. Comparative *in vitro* and *in vivo* assessment of toxin neutralization by anti-tetanus toxin monoclonal antibodies. *Human Vaccines Immunotherapeutics* 2014;10:344–51. <https://doi.org/10.4161/hv.26769>.
- [52] Vance DJ, Tremblay JM, Rong Y, Angalakurthi SK, Volkin DB, Middaugh CR, et al. High-resolution epitope positioning of a large collection of neutralizing and nonneutralizing single-domain antibodies on the enzymatic and binding subunits of ricin toxin. *Clin Vaccine Immunol* 2017;24. <https://doi.org/10.1128/CVI.00236-17>.
- [53] Chow SK, Smith C, MacCarthy T, Pohl MA, Bergman A, Casadevall A. Disease-enhancing antibodies improve the efficacy of bacterial toxin-neutralizing antibodies. *Cell Host Microbe* 2013;13:417–28. <https://doi.org/10.1016/j.chom.2013.03.001>.
- [54] Hernandez LD, Kroh HK, Hsieh E, Yang X, Beaumont M, Sheth PR, et al. Epitopes and mechanism of action of the clostridium difficile Toxin A-neutralizing antibody actoxumab. *J Mol Biol* 2017;429:1030–44. <https://doi.org/10.1016/j.jmb.2017.02.010>.
- [55] Herrera C, Klokk TI, Cole R, Sandvig K, Mantis NJ. A bispecific antibody promotes aggregation of ricin toxin on cell surfaces and alters dynamics of toxin internalization and trafficking. *PLoS ONE* 2016;11:e0156893. <https://doi.org/10.1371/journal.pone.0156893>.
- [56] Montal M. Tetanus neurotoxin: conformational plasticity as an adaptive strategy. *EMBO Rep* 2017;18:1268–70. <https://doi.org/10.15252/embr.201744500>.
- [57] Lam KH, Tremblay JM, Vazquez-Cintrón E, Perry K, Ondeck C, Webb RP, et al. Structural insights into rational design of single-domain antibody-based antitoxins against botulinum neurotoxins. *Cell Rep*. 2020;30(2526–39):e6. <https://doi.org/10.1016/j.celrep.2020.01.107>.
- [58] Schmidt DJ, Beamer G, Tremblay JM, Steele JA, Kim HB, Wang Y, et al. A Tetraspecific VHH-based neutralizing antibody modifies disease outcome in three animal models of clostridium difficile infection. *Clin Vaccine Immunol* 2016;23:774–84. <https://doi.org/10.1128/CVI.00730-15>.
- [59] Yang Z, Schmidt D, Liu W, Li S, Shi L, Sheng J, et al. A novel multivalent, single-domain antibody targeting TcdA and TcdB prevents fulminant Clostridium difficile infection in mice. *J Infect Dis* 2014;210:964–72. <https://doi.org/10.1093/infdis/jiu196>.
- [60] Spaun J, Lyng J. Replacement of the international standard for tetanus antitoxin and the use of the standard in the flocculation test. *Bull World Health Organ* 1970;42:523–34.
- [61] Farrar JJ, Yen LM, Cook T, Fairweather N, Binh N, Parry J, et al. Tetanus. *J Neurol Neurosurg Psychiatry* 2000;69:292–301. <https://doi.org/10.1136/jnnp.69.3.292>.
- [62] Dewey CW, Myopathies Talarico LR. disorders of skeletal muscle. Chapter 18. In: Dewey CW, editor. *A practical guide to canine and feline neurology*. Wiley Blackwell Publishing; 2016.
- [63] Harmsen MM, Fijten HPD, Engel B, Dekker A, Eblé PL. Passive immunization with llama single-domain antibody fragments reduces foot-and-mouth disease transmission between pigs. *Vaccine* 2009;27:1904–11. <https://doi.org/10.1016/j.vaccine.2009.01.110>.
- [64] Tremblay JM, Mukherjee J, Leysath CE, Debatis M, Ofori K, Baldwin K, et al. A single VHH-based toxin-neutralizing agent and an effector antibody protect mice against challenge with Shiga toxins 1 and 2. *Infect Immun* 2013;81:4592–603. <https://doi.org/10.1128/IAI.01033-13>.
- [65] Chapeton-Montes D, Plourde L, Bouchier C, Ma L, Diancourt L, Criscuolo A, et al. The population structure of Clostridium tetani deduced from its pan-genome. *Sci Rep* 2019;9:11220. <https://doi.org/10.1038/s41598-019-47551-4>.
- [66] Barkoff AM, Mertsola J, Pierard D, Dalby T, Hoegh SV, Guillot S, et al. to 2015. *Euro Surveill* 1998;2019:24. <https://doi.org/10.2807/1560-7917.ES.2019.24.7.1700832>.
- [67] Xu Y, Wang D, Mason B, Rossomando T, Li N, Liu D, et al. Structure, heterogeneity and developability assessment of therapeutic antibodies. *mAbs*. 2019;11:239–64. <https://doi.org/10.1080/19420862.2018.1553476>.